Nuclear Engineering and Design 239 (2009) 2317–2325

Contents lists available at ScienceDirect

Nuclear Engineering and Design

journal homepage: www.elsevier.com/locate/nucengdes

Study on the characteristic points of boiling curve by using wavelet analysis and genetic neural network

H.M. Wei, G.H. Su*, W.X. Tian, S.Z. Qiu, W.F. Ni

Department of Nuclear Science and Technology, State Key Laboratory of Multiphase Flow in Power Engineering, Xi'an Jiaotong University, 710049, Xi'an, China

ARTICLE INFO

Article history:
Received 28 October 2008
Received in revised form 21 June 2009
Accepted 6 July 2009

Keywords:
Genetic algorithm
Wavelet analysis
Genetic neural network
Prediction

ABSTRACT

Local singularity of a signal includes a lot of important information. Wavelet transform can overcome the shortages of Fourier analysis, i.e., the weak localization in the local time- and frequency-domains. It has the capacity to detect the characteristic points of boiling curves. Based on the wavelet analysis theory of signal singularity detection, Critical Heat Flux (CHF) and Minimum Film Boiling Starting Point (q_{min}) of boiling curves can be detected by using the wavelet modulus maxima detection. Moreover, a genetic neural network (GNN) model for predicting CHF is set up in this paper. The database used in the analysis is from the 1960s, including 2365 data points which cover a range of pressure (P), from 100 to 1000 kPa, mass flow rate (G) from 40 to 500 kg m^{-2} s^{-1}, inlet sub-cooling (ΔT_{sub}) from 0 to 35 K, wall superheat (ΔT_{sat}) from 10 to 500 K and heat flux (Q) from 20 to 8000 kW m^{-2}. GNN mode has some advantages of its global optimal searching, quick convergence speed and solving non-linear problem. The methods of establishing the model and training of GNN are discussed particularly. The characteristic point predictions of boiling curve are investigated in detail by GNN. The results predicted by GNN have a good agreement with experimental data. At last, the main parametric trends of the CHF are analyzed by applying GNN. Simulation and analysis results show that the network model can effectively predict CHF.

1. Introduction

In general, local singularity of a signal includes a lot of important information. Wavelet transform can overcome the shortages of Fourier analysis, i.e., the weak localization in the local time- and frequency-domains. It has the good localization characteristic to study the singularity of boiling curves. It has been applied widely in the theory and the practice.

It is well known that the boiling curve reflects the relation between wall superheat and heat flow. In general, these boiling curves do not always include nucleate boiling, transition boiling and film boiling regions, as shown in Fig. 1. They often show just one or two of the three parts. The CHF and Minimum Film Boiling Starting Point (q_{min}) of boiling curves can be detected by using the wavelet multi-resolution analysis. CHF is one of the most important quantities when considering the safety limits of nuclear reactors, steam generators, and other thermal units. It cannot increase indefinitely. In some cases, the steam produced leads to the formation of a continuous vapor film over the surface which may cause the destruction of the heater due to a sudden increase of the surface temperature. The pressurized water nuclear reactors must be designed with sufficient thermal (power) margin for the specifically acceptable fuel design limits to ensure that they are operated safely within the limiting conditions for operation. The limitation is produced from the analysis of CHF. So the detection of characteristic points of boiling curve is very important.

In this study, we employ the local modulus maxima of cubic B-spline wavelet transform to determine the location of CHF. Daubechies wavelets and B-spline wavelets have been dominantly used in wavelet analysis. Compared to Daubechies wavelets, the compactly supported cardinal B-spline wavelets have several distinctive desirable properties including small support of scaling functions and wavelets, total positivity of the scaling functions, easy construction and fast implementation (Dubieties, 1988; Chui, 1992).

The prediction of CHF is most crucial in designing various transfer units including nuclear reactors fossil-fueled boilers, fusion devices, and so on. When CHF occurs, the heat transfer capability decreases dramatically and the corresponding wall temperature increases rapidly that it can even melt the heat transfer surface (Wang et al., 2000). The power generated is often limited by the CHF value. It is an important parameter to be predicted in safety analysis of nuclear power system. Therefore, the research on CHF has been extensively carried out during the last four decades.

GA is a stochastic search algorithm (Guo et al., 2000; Goldberg, 1989) inspired by the mechanics of natural evolution. Goldberg

* Corresponding author. Tel.: +86 29 82663401; fax: +86 29 82663401.
E-mail address: ghsu@mail.xjtu.edu.cn (G.H. Su).

0029-5493/$ – see front matter © 2009 Elsevier B.V. All rights reserved.
doi:10.1016/j.nucengdes.2009.07.016

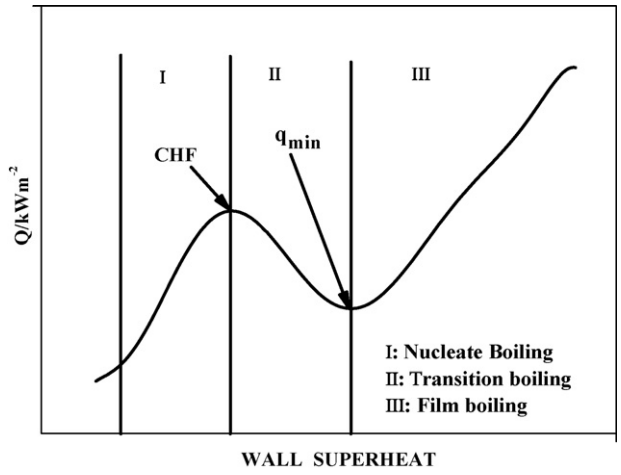

Fig. 1. Schematic diagram for flow boiling curves.

(1989) and Michalewicz (1992) discussed the mechanism and robustness of GA in solving non-linear optimization problems. Compared to the conventional optimization methods that move from one point to another, GA starts from many points simultaneously climbing many peaks in parallel (Misra and Sharma, 1991). Therefore, GA is less susceptible to be stuck at local minima than conventional search methods (Goldberg, 1989; Mitchell, 1996). It is one of the strategic randomized search techniques, which are well known for its robustness in finding the optimal or near optimal solution. The basic genetic operators are selection, crossover and mutation. Natural selection increases the surviving capability of the populations over the foregoing generations. Crossover is the recombination of the information from two good 'parent' solutions into what we hope are even better 'offspring' solutions. Mutation promotes diversity at random and explores more global areas of the solution space providing a mechanism to escape from local optima. Then, from generation to generation, the average fitness of the individuals increases, evolving the population to its optimum adaptation. The new chromosomes reproduced by selection, crossover and mutation operators were evaluated, and this procedure for evaluation and reproduction of all chromosomes was repeated until the stopping criterion is satisfied. A complete description of GA can be given in Shopova and Vaklieva-Bancheva (2006).

BP neural network model is a kind of learning algorithms used to transfer oppositely from former to multi-level neural network. It can simulate any non-linear function. It has been widely used in many applications (Liang et al., 2000; Looney, 1997). However, there are some shortcomings for BP neural network during the training course, such as slow training speed and easily get stuck into local minimum. This is very disadvantageous under finite experiment data of CHF. So in order to improve the training speed and reliability of network, the present paper adopts a method to integrate genetic algorithm and neural network. GA was used to optimize the weight and threshold of BP neural network (Adineh et al., 2008; Motlaghi et al., 2008; Sahoo and Ray, 2006). The shortcoming is solved and the weight and threshold are optimized, thus the accurate degree of predicting CHF data is achieved by GNN.

The aim of this study is to propose some methods to detect and predict the characteristic points of boiling curves. Wavelet analysis has the good localization characteristic in studying boiling curves. It is employed to detect the characteristic points of boiling curves. The GNN mode has some advantages including its global optimal searching, quick convergence speed and solving non-linear problem. It is used to predict the characteristic points. The data from the past four decades have been tabulated in Table 1, respectively. In this paper, at first, we introduce the basic theories of the two methods—wavelet modulus maxima detection and GNN. Secondly, the locations of characteristic points of boiling curves are determined by using the local modulus maxima detection of cubic B-spline wavelet transform. The experimental data of characteristic points of boiling curves are used to train and test the network. Next, the characteristic points of boiling curves are predicted by GNN. We give the comparisons between the experimental data and GNN prediction. The prediction results of the characteristic points of boiling curves are consistent with experimental data very well. Approximately 98% of the data were predicted within the ±10% error range. At last, the effects such as pressure, mass flow rate and inlet sub-cooling of main parameters on CHF are analyzed by using the GNN. The results agree with practical behavior as they are generally understood.

2. Singularity detection of wavelet analysis

Wavelet analysis is a kind of methods that have the characteristics of time-frequency analysis. Comparing with Fourier analysis, wavelet analysis overcomes the weakness of analyzing signals only in frequency-domain (Mallat, 1989). Generally, the wavelet transform can be realized. Wavelet analysis is the best choice for analyzing complex non-linear signals (Mallat and Hwang, 1992). At present, wavelet analysis has been applied in the research of two-phase flow widely and successfully. The singular point of signal may

Table 1
Database of flow boiling.

Reference	Test section	Working fluid	Parameter range
Chen et al. (1979)	Stainless steel and Inconel; circular duct (tube); D_O = 19.1 and 15.9 δ=1.65, 0.89 and 1.02 L = 4, 3.5	Water	P = 0.1, G = 100–400, ΔT_{sub} = 10–80, T_w = 270–800
Ragheb et al. (1981)	D_O = 13.1 and δ = 0.559 for Zircaloy; D_O = 14.0 and δ = 0.635 for Al; D_O = 12.7 and δ = 0.38 Inconel; D_O = 12.7 and δ=0.38 for Cu; tube	Water	P = 0.1, G = 68–203, ΔT_{sub} = 0–28,
Wang and Seban (1988)	D_O = 16.1, δ = 0.8, L = 3.66; tube	Water	P = 0.1–0.4, G = 25–75, ΔT_{sub}=33–81
Huang et al. (1994)	Monel; D_O = 10, δ = 0.15, L = 0.05; tube	Water	P = 0.1–1.0, G = 25–500, ΔT_{sub} = 5–50
Ragheb and Cheng (1979)	D_O = 12.7; tube	Water	P = 0.1, G = 34–102, ΔT_{sub} = 0–28
Huang et al. (1993)	Ni; D_O = 32, δ = 5.575, L = 0.05; tube	Water	P = 0.1–1.0,G = 100–200, ΔT_{sub} = 30
Huang et al. (1993)	Cu; D_O = 32, δ = 11, L = 0.05; tube	Water	P = 0.1–1.2, G = 25–500, ΔT_{sub} = 3–30
Cheng et al. (1977)	Cu; D_O = 95.3, δ = 41.3, L = 0.0572; tube	Water	P = 0.1, G = 136, ΔT_{sub} = 0
Cheng et al. (1978a)	Cu, D_O = 95.3, δ = 41.3, L = 0.0572; tube	Water	P = 0.1, G = 68–203, ΔT_{sub} = 0–28
Cheng et al. (1978b)	Cu, D_O = 95.3, δ = 41.3, L = 0.0572; tube	Water	P = 0.1, G = 136, ΔT_{sub} = 0–28
He (1989)	Stainless steel, D_O = 16, δ = 2, L = 0.1; tube	Water	P = 0.117–2.9, G = 40.8–123, ΔT_{sub} = 9.1–26.3
Qian et al. (1994)	Stainless steel, D_O = 20, δ = 2, L = 1; tube	Water	P = 0.25–1.09, G = 74.2–223.9, ΔT_{sub} = 5.5–32.4

Note. D_O, tube outside diameter (mm); δ, tube wall thickness (mm); L, tube length (m); P, pressure (MPa); G, mass flow rate (kg m^{-2} s^{-1}); ΔT_{sub}, inlet sub-cooling (°C); T_w, initial wall temperature (°C).

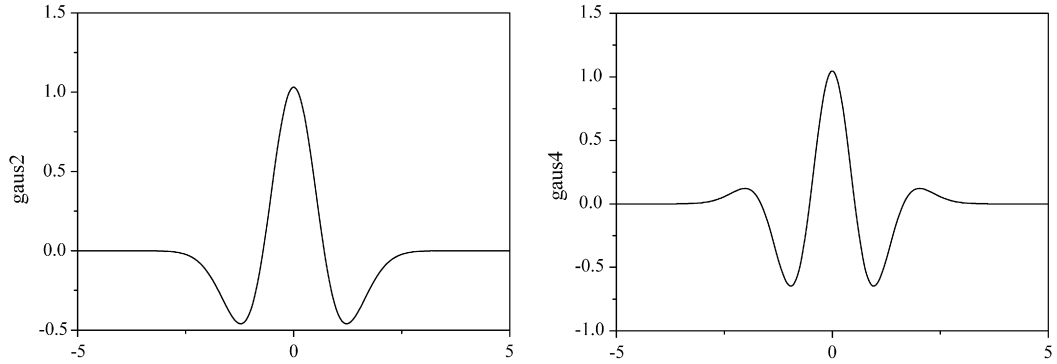

Fig. 2. Gauss wavelet.

be determined by using wavelet multi-scale edge detecting technology. At first, the original signal can be smoothed by means of various measures. Secondly, the singular point can be located according to the first derivation or the second derivation of the smooth signal. The modulus maxima point of the first derivation of smooth signal or the zero cross point of the second derivation of smooth signal is the corresponding singular point of original signal.

Supposing that $\theta(x)$ is smooth function, subject to

$$\int_{-\infty}^{\infty} \theta(x)dx = 1 \tag{1}$$

$$\lim_{x\to\pm\infty} \theta(x) = 0 \tag{2}$$

The edge detection wavelet of smooth function $\theta(x)$ can be constructed as following:

$$\psi^I(x) = \frac{d\theta(x)}{dx},\ \psi^{II}(x) = \frac{d^2\theta(x)}{dx^2} \tag{3}$$

Set $f(x)$ is original signal (Mallat and Hwang, 1992; Cheng, 1998), and its wavelet transform is obtained

$$W_s^I f(x) = f(x) * \psi_s^I(x) = f * \left(s\frac{d\theta_s}{dx}\right)(x) = s\frac{d}{dx}(f * \theta_s)(x) \tag{4}$$

$$W_s^{II} f(x) = f(x) * \psi_s^{II}(x) = f * \left(s^2\frac{d^2\theta_s}{dx^2}\right)(x) = s^2\frac{d^2}{dx^2}(f * \theta_s)(x) \tag{5}$$

where $\theta_s(x) = 1/s\theta(x/s)$, s is scale factor. If $\theta_s(x)$ is Gauss function, the zero cross detection is the known Marr–Hildreth edge detection (Ling and Kim, 1992) and the modulus maxima detection is the Canny edge detection (Canny, 1986; Mallat and Hwang, 1992). The sketches of the second- and four-orders Gauss function (smoothed function) are shown in Fig. 2. The convolution is defined as follows:

$$(f * g)(x) = \int_{-\infty}^{\infty} f(x-y)g(y)dy$$

where f, g are two functions and $f, g \in L^1(R)$. When f, g are discrete series, the convolution can be rewritten as:

$$w(m) = \sum_{n=-\infty}^{+\infty} f(n)g(m+1-n)$$

where $w(m)$ is the mth element of convolves f and g.

In the modulus maxima detection, the modulus maxima and minimum points are the sharp and slow change points, respectively. In the zero cross detection, the sharp and slow change points are all zero cross points. It is difficult to distinguish the sharp and slow change point. Therefore, we choose the modulus maxima detection to detect the sharp change characteristic points in this study.

Singularities are detected by finding the abscissa where the wavelet modulus maxima converge at fine scales. For fast numerical computations, the detection of wavelet transform maxima is limited to dyadic scales $s = \{2^j\}, (0 < j \le \log_2 N$, j is the wavelet hierarchy, and N is the length of signal). At each scale $s = 2^j$, the maxima representation provides the values of $W_s^I f(x)$ where $\left|W_s^I f(x)\right|$ is locally maximum. As the scale s increases, the small changes of boiling curves are eliminated by the convolution $\theta_{2^j} * f(x)$. So the big changes of boiling curves may be detected. The different sharp points of boiling curves can be detected at different scales. The finest scale can be determined by experiment. Fig. 3 can explain the modulus maxima and zero cross detection of the original signal $f(x)$. $\theta_{2^j} * f(x)$ is the signal of $f(x)$ smoothed by θ_{2^j}. Wavelet modulus maxima are the maxima of the first derivative of $f(x)$ smoothed by θ_{2^j}, as illustrated by $(d/dx)\theta_{2^j} * f(x)$. x_0 and x_2 are the sharp change points. Zero cross points are the zero points the second-order derivative of $f(x)$ smoothed by θ_{2^j}, as illustrated by $(d^2/dx^2)\theta_{2^j} * f(x)$.

3. GNN theory

3.1. Structure of the network

A multiple layer feed-forward and back-propagation neuron network is established to predict CHF. Input layer of the prediction network is responding to CHF parameter. The dimension of input layer can be completely designed according to influence factors on CHF. Output layer of the network is the CHF that will be predicted. The number of hidden layer unit is in direct contact with the predicting precision. Actually, the network with less number of hidden layer units will not be trained or not be strong enough to distinguish the sample that has never been learned, and also has lower general capacity. However, if the number of hidden layer unit is too much, training time will be prolonged and prediction error may

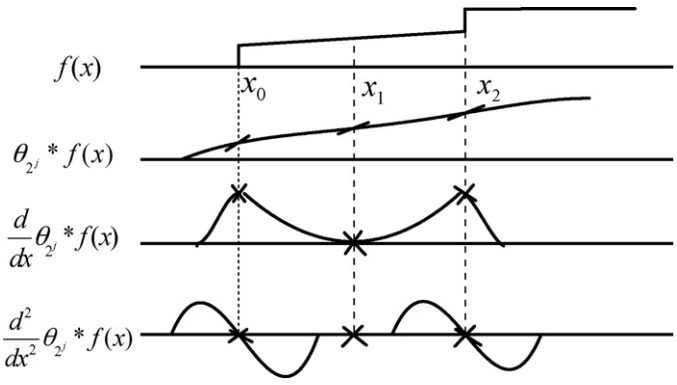

Fig. 3. The modulus maxima and zero cross detection of signal.

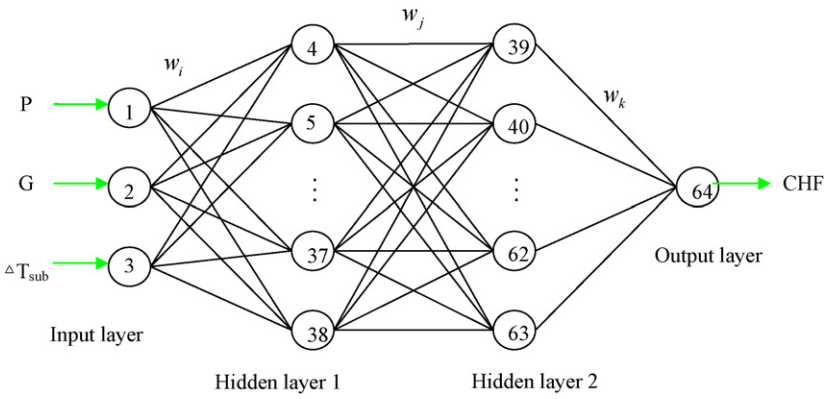

Fig. 4. GNN structure.

not be the minimum. Therefore, there must be the best number of hidden layer unit. The initial number of hidden layer unit is determined by using experiential method. In this study, the dimensions of input layer are 3. They are system pressure, mass flow rate and inlet sub-cooling, respectively. The dimension of output layer is 1. It is CHF. The first and second hidden layer units are 35 and 25, respectively. Therefore, a double hidden layers BP network can be constructed to predict the CHF. The topological structure of GNN with two hidden layers is shown in Fig. 4. The model of each neuron in the GNN includes non-linearity at the output end. The hyperbolic tangent function in hidden layers is used as transfer function. The transfer function in output layer is linear transfer function. Multilayer perception is trained in a supervised manner with a highly popular algorithm known as the back-propagation algorithm. This algorithm is based on the error-correction learning rule. The error back-propagation processes consist of two passes through the different layers of the network: forward pass and backward pass. In the forward pass, an input vector is applied to the sensory nodes of the network, and its effect propagates through the network, layer by layer. During the backward pass, the synaptic weights are all adjusted in accordance with the error-correction rule. The actual response of the network is subtracted from a desired response to produce an error signal. This error signal is then propagated backward through the network and the synaptic weights are adjusted so as to make the actual response of the network move closer to the desired response. GNN consist of 60 neurons which are connected to one another. A neuron is an information-processing unit that is fundamental to the operation of a neural network. Fig. 5 shows the model for a neuron. In mathematical terms, a neuron is described by the following equation:

$$\text{output} = F\left(\sum_{k=1}^{p} w_k x_k + \theta\right) \tag{6}$$

where $x_1, x_2, \ldots, x_p$ are the input signals. $w_1, w_2, \ldots, w_p$ are the synaptic weights of neuron. θ is threshold and $F(\cdot)$ is the activation function which could have several forms, regarding the problem.

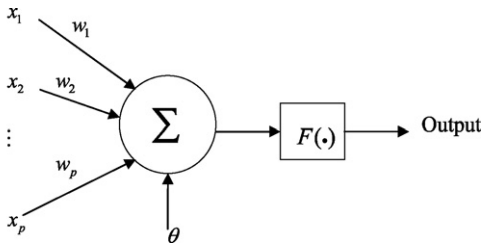

Fig. 5. Neuron model.

3.2. Optimizing network weight and threshold using GA

The GA is the most useful method (Ghorbani et al., 2007; Peng and Ling, 2008; Shin and Han, 2000; Xu, 2007) to solve optimization problems with multiple objectives. Genetic operation is an optimization algorithm that imitates the evolution process of natural principles, and develops quickly. This operation using colony search technology, which can be avoided getting into local extreme point, and can solve how to optimize weight and threshold of BP network. For a more thorough description of genetic algorithms we refer to Goldberg (1989). Genetic operation is employed to optimize the weight and threshold of the network in this study. The detailed operation is given as follows:

3.2.1. Coding of weight and threshold

The genetic operation is used to optimize the weight and threshold of the network and its input signals should be transformed into genetic genes—chromosome. The model adopts binary coding method. The vector that chromosome responding with weight and threshold of network is:

$$W = [W_1, \ldots, W_i, \ldots, \theta_1, \ldots, \theta_j] \tag{7}$$

where W_i is the ith weight gene of chromosome, θ_j is the jth threshold gene of chromosome.

3.2.2. Initialization of population

After coding the weight and threshold of the network, chromosome is yielded at random and makes up an initial population. And then we start iterative search using initial population as a start point. The initial weight and threshold can be obtained by random reactor. Initial population is made up of M bunches; each bunch is made up of weight and threshold and produces random. Finally, population size, selection probability, crossover probability and mutation probability are determined by experiments. The population size, selection probability, crossover probability and mutation probability are 100, 0.85, 0.56 and 0.0001, respectively.

3.2.3. Fitness function

Fitness function is an important principle on evaluating individual. All individuals are evaluated in terms of their performances, which is based on their fitness values. The chromosome with large fitness is reserved, and the small one is removed. The fitness function of the model uses the reciprocal of error squaring sum between prediction signal and goal signal, is as follows:

$$F_{\text{fitness}} = \frac{1}{\left(\left(\sum_{i=1}^{n}(A_i - T_i)^2\right)/n(n-1)\right) + \varepsilon} \tag{8}$$

where n stands for the number of the samples, A_i is prediction signal, and T_i is goal signal. The ε is 0.00001 in this study.

3.2.4. Selection operation

The selection operation for GA is the basic engine of Darwinian natural selection and survival of the fittest. The selection operation is to choose the individual who has the strongest vitality from the population, and it has the chance to propagate offspring. Selection is done according to the natural principia of "good win and bad lost", that is, individual with large fitness will be reserved and the opposite one will be removed. A stochastic universal sampling method is used to choose new individual in this study. Probability of individual selection is:

$$P_i = \frac{F_i}{\sum_{i=1}^{n} F_i} \tag{9}$$

where, P_i and F_i are the selection probability and fitness of ith individual, respectively. The weight and threshold of the network gradually approach to optimal values through selection operation. In the learning process, the largest fitness individual is reserved for offspring.

3.2.5. Crossover operation

The crossover operator creates two new chromosomes from two existing chromosomes by cutting them at a random position and exchanging the parts following the cut. It starts with two parental chromosomes and produces two offspring chromosomes. In this study, two parental chromosomes and bunch's crossing position are determined by random. And then their bunches are exchanged behind crossing point of parental chromosome and produce two new offspring chromosomes, these two new chromosomes have their parental feature.

3.2.6. Mutation operation

Mutation introduces innovation into the chromosomes. It is a genetic operator that alters one ore more gene values in a chromosome from its initial state. It increases the variability of the chromosomes and helps to avoid the possibility of falling into local optima in the evolution process (Krishnakumar and Goldberg, 1992). In this work, the non-uniform mutation (Cook et al., 2000) is chosen. From one generation to the next, the chromosomes have a better fitness (Paris and Pierreval, 2001). By using the above genetic algorithm operation, appropriate network weight and threshold are obtained. The GA optimization, training, learning and prediction procedure for the CHF data is represented in Fig. 6.

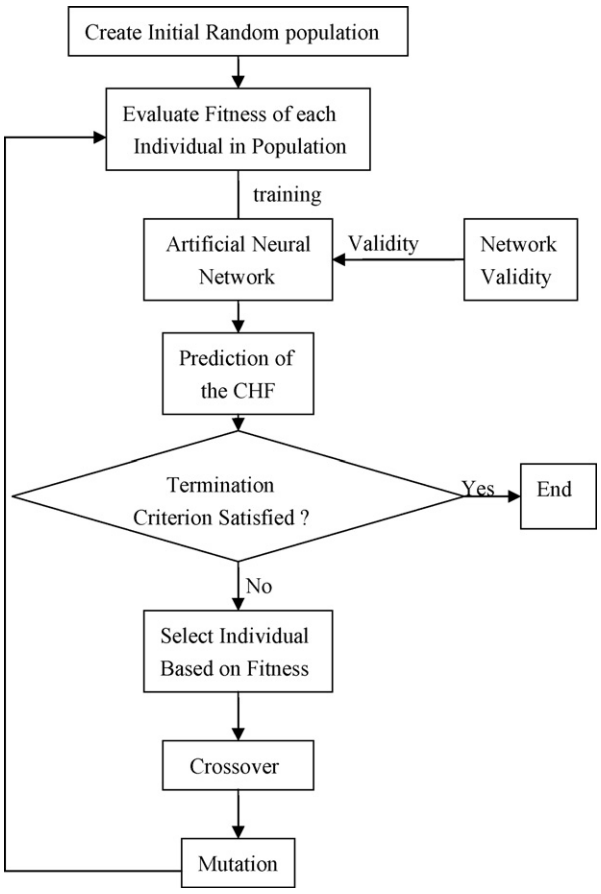

Fig. 6. The overall prediction procedure for the CHF database.

4. CHF determination

The wavelet modulus maximum method is applied to detect the singularity of the pressure fluctuations in a circulating fluidized bed (Chen et al., 2004). This method has been tested effective under various operation conditions. The wavelet modulus maximum is used to detect the spike wave of epileptic EEG (electroencephalogram) signals by detecting their singular points (Shen et al., 1998). Results show that the spike detection rate is 94.2%, and no false detection for normal EEG signals. Shang et al. (2001) applied the wavelet modulus maximum to detect the faults in high-voltage direct current (HVDC) system. Their simulation results show that the wavelet modulus maximum can make a definite identification of HVDC line faults. Yue et al. (2009) pointed out that the wavelet modulus maximum could effectively detect the polarity of non-effectively earthed neutral system. In flow boiling heat transfer regime, the temperature of the fluid is on the saturated level and the wall temperature also keeps nearly a constant value. However, when CHF occurs, the corresponding wall temperature increases rapidly. Using previous methods, the location of CHF can be observed with the rapid change of temperature by using the thermocouples arranged in the test section. In fact, the location of CHF may be occurring before (or behind) the observed position. In mathematics, it can be represented by a larger singularity on that point. The CHF and Minimum Film Boiling Starting Point are the singularity points of boiling curves. The wavelet has the capacity to detect the singularity points of boiling curves. So in this work, it is employed to determine the location of CHF. It may accurately determine the location of the characteristic points of boiling curves by an intelligent way of interpolating though old data points. The location of CHF can then be detected according to the rapid change in temperature.

The results are different to process the same problem by using different wavelet functions. It is very important to choice the finest smooth function (i.e., wavelet function) in practical application. The choice criteria of wavelet function are determined by its compactly supported, symmetry, vanishing moment and regularity. The length of wavelet function is determined by compactly supported length. It reflects the local ability of wavelet. The symmetry may effectually guarantee linear phase. The ability of wavelet approximations to smooth function increases with increasing vanishing moment. Because of the good regularity of wavelet, it is easy to obtain smooth reconstruction curves. Above all, the four-order B-spline wavelet ψ_4 is used as smooth function. It is given as follows:

$$\psi_4 = \begin{cases} x^3/6, & 0 \le x < 1; \\ -x^3/2 + 2x^2 - 2x + 2/3, & 1 \le x < 2; \\ x^3/2 - 4x^2 + 10x - 22/3, & 2 \le x < 3; \\ (4-x)^3/6, & 3 \le x < 4; \\ 0, & \text{else.} \end{cases}$$

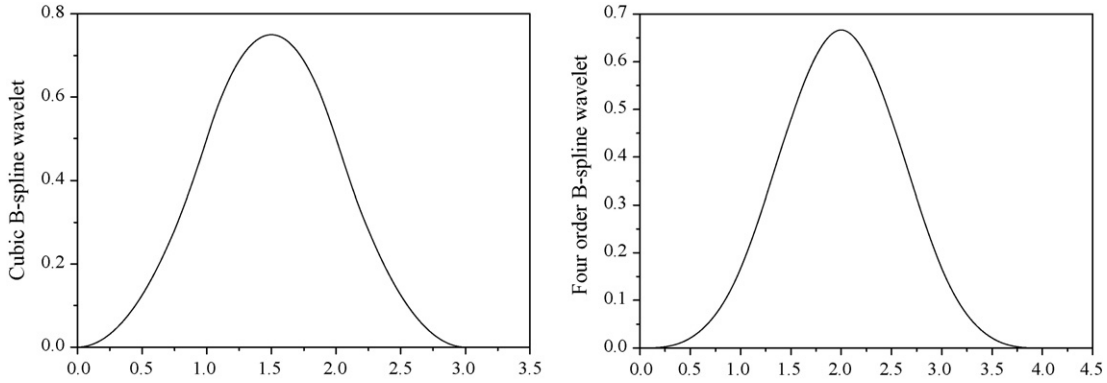

Fig. 7. B-spline wavelet.

So the cubic B-spline wavelet is employed to detect the singularities of boiling curves. The sketches of the cubic and four-order B-spline wavelets are shown in Fig. 7.

In the following text, we give the detection result. The boiling curve obtained from experiment is shown in Fig. 8. The result of wavelet modulus maxima detection is showed in Fig. 9. From Fig. 9, we can clearly see two modulus maxima points: the one is the CHF point, the other is the Minimum Film Boiling Starting Point (q_{min}) of boiling curves. So we can accurately determine the locations of the characteristic points of boiling curves. CHF occurred only at wall superheat of 48.89 K. The Minimum Film Boiling Starting Point (q_{min}) occurred only at wall superheat of 158.49 K. Figs. 10–12 show the comparison between detection results and experimental data for CHF, q_{min} and wall superheat corresponding to q_{min}, respectively. From the results, the root-mean-square (RMS) errors of the detection results are 4.72, 5.84 and 6.94%, respectively. From Figs. 10–12, we can clearly know that the detection results by wavelet modulus maxima detection have a good agreement with experimental data. Our results show that wavelet analysis can accurately detect the characteristic points of boiling curves.

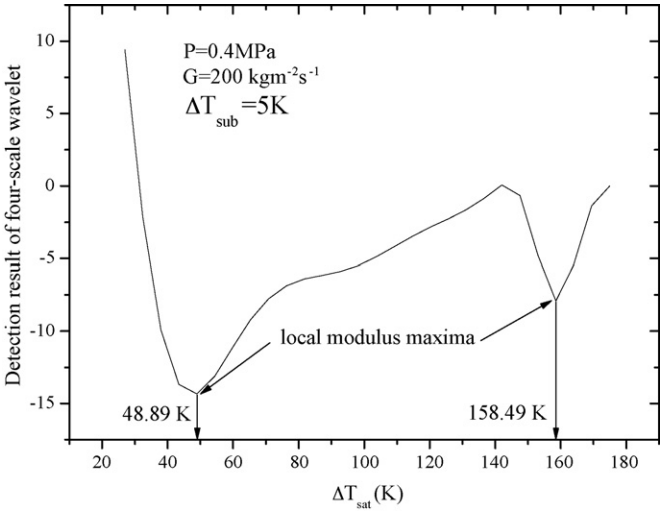

Fig. 9. Wavelet detection result.

5. Prediction of the characteristic points

The prediction of CHF is most crucial in designing various transfer units including nuclear reactors fossil-fueled boilers, fusion devices, and so on. When CHF occurs, the surface cooled is no longer in intimate contact with the liquid film. As a result, the heat transfer capability decreases so dramatically and the corresponding wall temperature rises so rapidly that it can even melt the heat transfer surface (Wang et al., 2000). The power generated is often limited by the CHF value. It is an important parameter to be predicted in safety analysis of nuclear power system. Therefore, prediction of characteristic points of boiling curves is investigated by GNN in this section. A double hidden layers BP

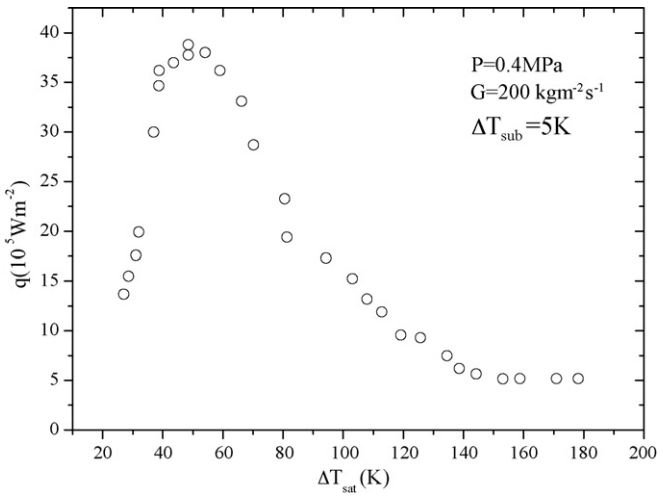

Fig. 8. Experimental boiling curve.

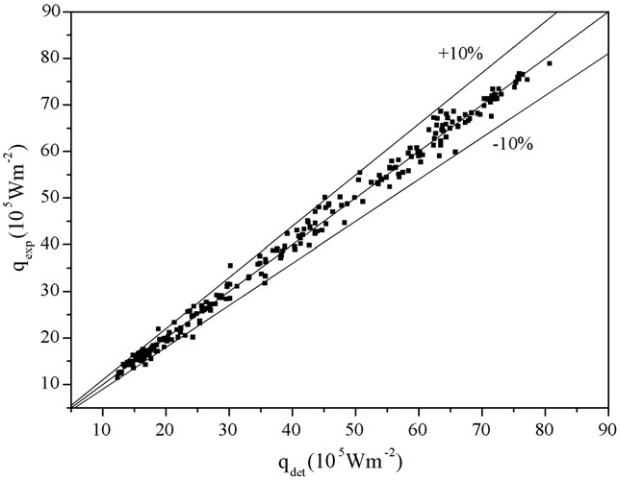

Fig. 10. Comparisons between the experimental data and wavelet detection results of CHF.

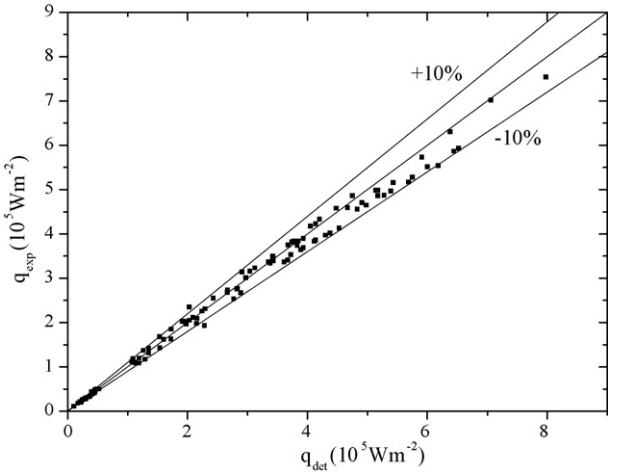

Fig. 11. Comparisons between the experimental data and wavelet detection results of q_{min}.

network is constructed to predict those characteristic points. The dimension of input layer is 3. They are pressure, mass flow rate and inlet sub-cooling, respectively. The dimension of output layer is 1. It is the CHF, q_{min} or wall superheat corresponding to q_{min}. The first and second hidden layer units are 35 and 25, respectively. The GNN is trained and tested based on those experimental data. From these, 70% of the experimental data was used for training and cross validation (60% for training and 10% for cross validation) and the rest 30% for testing the network. The mean square errors (MSE) of the training, validation and testing are all lower than 0.06319, 0.07912 and 0.08475, respectively. The trained GNN is used to predict CHF, q_{min} and wall superheat corresponding to q_{min}, respectively. The prediction results are shown in the following Figs. 13–15. Figs. 13–15 show the comparison between prediction results and experimental data for CHF, q_{min} and wall superheat corresponding to q_{min}, respectively. From Figs. 13–15, we can clearly know that the prediction results by GNN have a good agreement with experimental data. From the results, the root-mean-square (RMS) errors of the prediction results are 7.18, 6.24 and 12.5%, respectively. Our results show that an appropriately trained GNN can accurately predict the characteristic points of boiling curve.

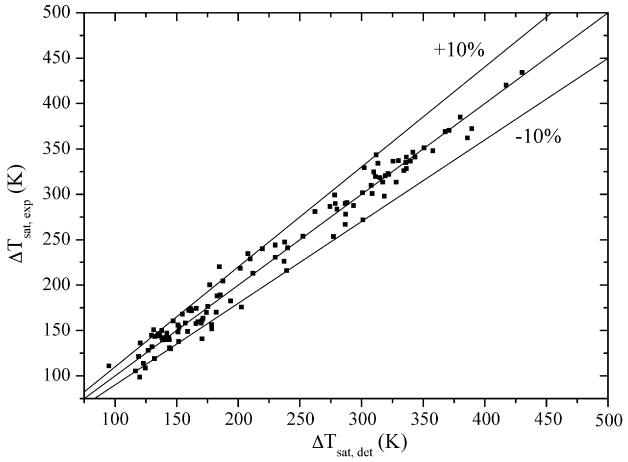

Fig. 12. Comparisons between the experimental data and wavelet detection results of wall superheat corresponding to q_{min}.

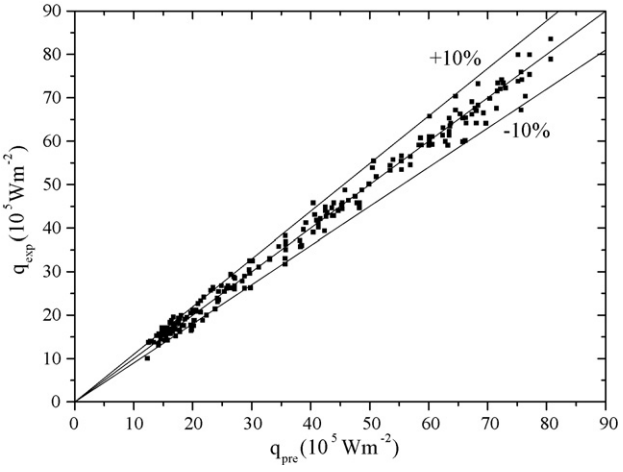

Fig. 13. Comparisons between the experimental data and GNN prediction results of CHF.

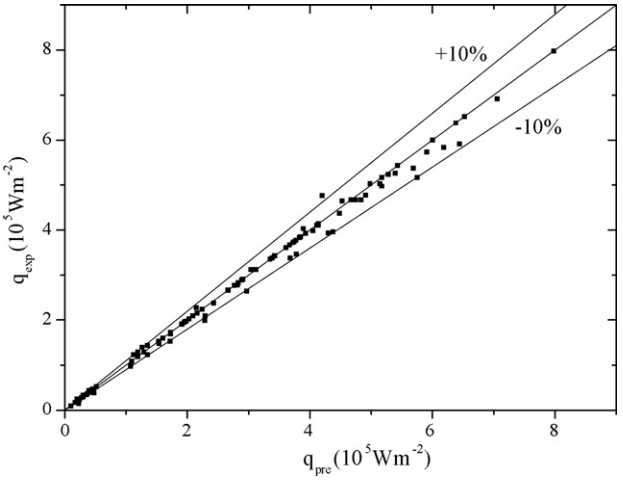

Fig. 14. Comparisons between the experimental data and GNN prediction results of q_{min}.

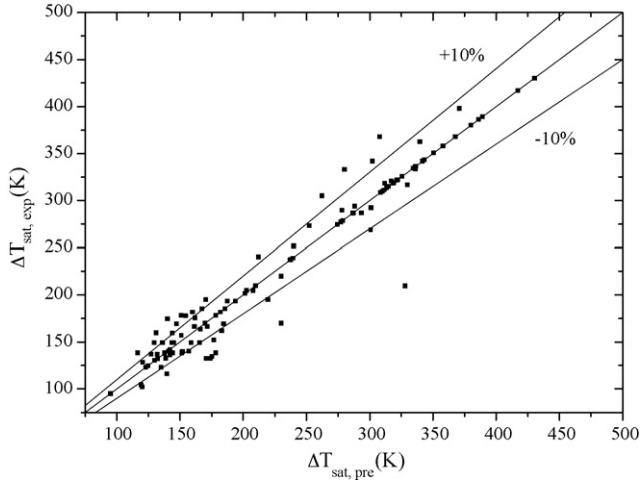

Fig. 15. Comparisons between the experimental data and GNN prediction results of wall superheat corresponding to q_{min}.

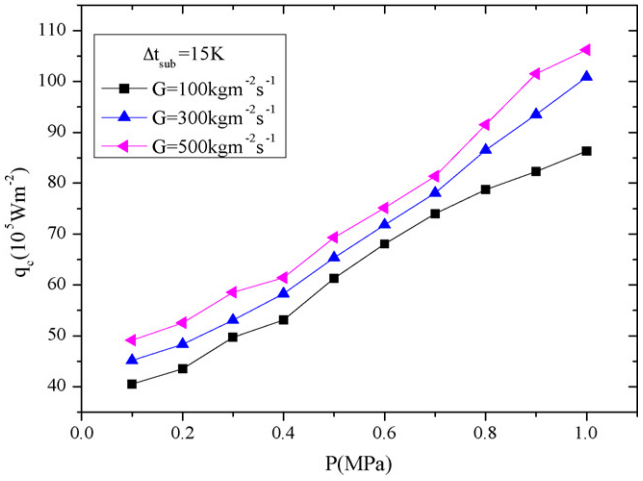

Fig. 16. Effect of system pressure on CHF.

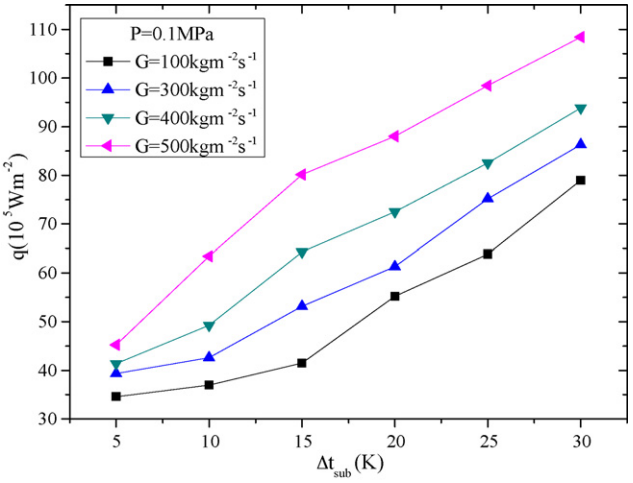

Fig. 18. Effect of inlet sub-cooling on CHF.

6. Parametric trends

An exact understanding of parametric trends is important in practical applications. In this section, the parametric trends based on fixed inlet conditions are predicted by using GNN. The fixed inlet conditions hypothesis is nearly independent of the other variable besides system pressure, mass flux and inlet sub-cooling. However, it is very useful for the prediction of the CHF in practical applications. The prediction parametric trends are shown in Figs. 16–18. In the figures, the actual outputs of the GNN are simply connected by lines. The trends agree with general understanding. The parametric trends are discussed as follows.

The overall trend of system pressure is shown in Fig. 16. Fig. 16 shows the variation of CHF with pressure under fixed inlet conditions. CHF data are represented for a fixed inlet sub-cooling of 15 K and different mass velocities in a pressure range of 0.1–1 MPa. From Fig. 16, we can clearly see that the CHF increases with increasing system pressure under low pressures.

The effects of mass flow velocity on CHF under different system pressures are illustrated in Fig. 17 for a fixed inlet sub-cooling of 15 K in a broad mass flow velocity range of 50–500 kg m^{-2} s^{-1}. Fig. 17 shows the CHF increases with increasing mass flow velocity at low mass flow velocity. From Fig. 17, we can also see that the CHF increases with increasing the system pressure.

The overall trend of inlet sub-cooling is shown in Fig. 18. The effects of inlet sub-cooling on CHF at different mass flow velocities

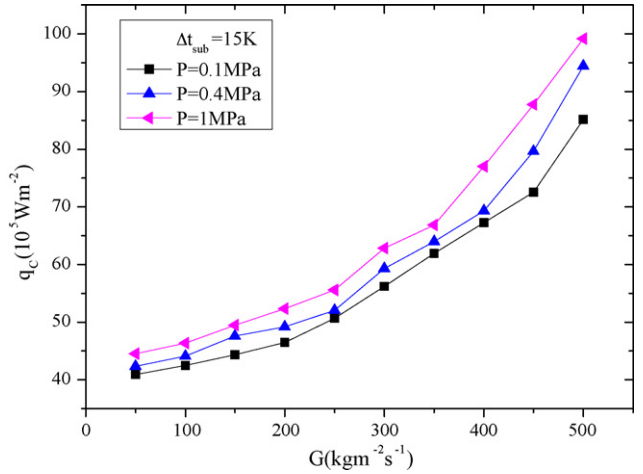

Fig. 17. Effect of mass flow velocity on CHF.

are represented in Fig. 18 for a fixed system pressure of 0.1 MPa. In this figure, the results can be obtained by the GNN. In overall, the CHF increases as the inlet sub-cooling increases for low inlet sub-cooling as shown in Fig. 18. From this figure, we can also clearly see that the trend of the mass flow velocities. The CHF increases with increasing mass flow velocity at low mass flow velocity.

Any way the occurrence of CHF is very complicated and there are several mature mechanism models. However all proposed models reveal that the DNB is relative with bubble dynamics and liquid film near the heating wall. In present study, the experimental range of system pressure is very limited and quite low, i.e., from 0.1 to 1.0 MPa, so it is not proper to draw a proper conclusion on the effect of pressure on CHF in such a limited range. Anyway, pressure plays a predominant role and improves heat transfer in all boiling regions. An increase in pressure obviously improves the heat transfer in boiling regions particularly at low pressure. So the prediction results show that the CHF will increase with an increase in pressure in present parametric range. For the effect of mass flux, higher mass flux obviously enhances the turbulence and it is much more difficult to generate bubble clusters. The mechanism of DNB is (1) rapid evaporation of liquid film between the bubble and heating wall or (2) accumulation of small bubbles near the heating surface and so on. The mechanism of MFBP is that a stable vapor film is attained near the heating surface. So it is well understandable that larger heat flux is necessary to generate DNB and MFBP at higher mass flux. For the effect of inlet sub-cooling degree, it can affect the local parameter (MNB or MFBP) more or less although many researchers believed that DNB is a 'local phenomenon'. Considering this memory effect, it is not difficult to understand that higher inlet sub-cooling results into a higher heat flux and temperature in DNB and MFBP.

7. Conclusions

Wavelet analysis and GNN are particularly discussed to analysis the characteristic points of flow boiling curves with a database composed of experimental data from the 1960s. The database includes 2365 data points that cover the following parameter ranges: pressure of 100–1000 kPa; mass flow rate of 40–500 kg m^{-2} s^{-1}; inlet sub-cooling of 0–35 K; wall superheat of 10–500 K and heat flux of 20–8000 kW m^{-2}.

The wavelet modulus maxima detection was applied successfully to detect the characteristic points of flow boiling curves. It has the good localization characteristic to study boiling curves. The detection results are shown in Figs. 10–12. From the results, we

can clearly know that the detection results by wavelet modulus maxima detection have a good agreement with experimental data. Our results show that wavelet analysis can accurately detect the characteristic points of boiling curves.

The GNN was applied successfully to predict the characteristic points of flow boiling curves. It applied genetic algorithm to optimize BP neural network weight and threshold. It overcomes some shortcomings of BP neural network, such as slow convergence and easily deep in local extreme point. It reduces experiment times and improves reliability of network. The prediction results are shown in the Figs. 13–15. The prediction results by GNN have a good agreement with experimental data. From the results, the proposed methodology allows accurate results to be achieved, thus the GNN is suitable for boiling curve data processing. The developed method can be used in numerous two-phase flow problems.

Finally, the effects of the main parameters on flow boiling curves are analyzed and the following result is obtained: the CHF increases with increasing system pressure, mass flow rate and inlet subcooling, respectively. It should be clear that these initial useful results on CHF in the nuclear plant applications are not sufficient for industrial standard, and that additional and more accurate results should be expected from further works.

Acknowledgments

This work is supported by the Program for New Century Excellent Talents in University (NCET-06-0837) and by the National Natural Science Foundation of China (No.10675096 and No. 19675028).

References

Adineh, V.R., et al., 2008. Optimization of the operational parameters in a fast axial flow CW CO_2 laser using artificial neural networks and genetic algorithms. Opt. Laser Technol. 40 (8), 1000–1007.
Canny, J., 1986. A computational approach to edge detection. IEEE Trans. PAMI 8 (6), 679–698.
Chen, W.J., et al., 1979. Measurement of boiling curves during rewetting of a hot circular duct. Int. J. Heat Mass Transfer 22, 973–976.
Chen, Y.G., et al., 2004. Detection of singularities in the pressure fluctuations of circulating fluidized beds based on wavelet modulus maximum method. Chem. Eng. Sci. 59, 3569–3575.
Cheng, S.C., et al., 1977. A technique to construct a boiling curve from quenching data considering heat loss. Int. J. Multiphase Flow 3, 495–499.
Cheng, S.C., et al., 1978a. Measurements of boiling curves of subcooled water under forced convective conditions. Int. J. Heat Mass Transfer 21, 1385–1392.
Cheng, S.C., et al., 1978b. Measurements of transition boiling data for water under forced convective conditions. J. Heat Transfer 100, 382–384.
Cheng, Z.X., 1998. Algorithm and Application of Wavelet Analysis. Xi'an Jiaotong University Press, Xi'an.
Chui, C.K., 1992. An Introduction to Wavelets. Academic Press.
Cook, D.F., et al., 2000. Combining a neural network with a genetic algorithm for process parameter optimization. Eng. Appl. Artif. Intell. 13 (4), 391–396.
Dubieties, I., 1988. Orthonormal bases of compactly supported wavelets. Comm. Pure Appl. Math. 41, 909–996.
Ghorbani, R., et al., 2007. Nearly optimal neural network stabilization of bipedal standing using genetic algorithm. Eng. Appl. Artif. Intell. 20 (4), 473–480.
Goldberg, D.E., 1989. Genetic Algorithms in Search Optimization and Machine Learning. Addison Wesley, Reading, MA.
Guo, Q., et al., 2000. Sequential projection pursuit using genetic algorithms for data mining of analytical data. Anal. Chem. 72, 2846–2855.
He, G.W., 1989. Transition Boiling Heat Transfer in a Vertical Tube. Master thesis of Xi'an Jiaotong University.
Huang, X.C., et al., 1993. Comparison of transient and steady-state boiling curves for forced upflow of water in a circular tube at medium pressure. Int. Commun. Heat Mass Transfer 20, 383–392.
Huang, X.C., et al., 1994. Quenching experiments with a circular test section of medium thermal capacity under forced convection of water. Int. J. Heat Mass Transfer 37, 803–818.
Krishnakumar, K., Goldberg, D.E., 1992. Control system optimization using genetic algorithms. J. Guid. Contr. Dynam. 15 (3), 735–739.
Liang, Y.C., et al., 2000. Proper orthogonal decomposition and its application—part II: model reduction for MEMS dynamical analysis. J. Sound Vib. 256, 515–532.
Ling, H., Kim, K., 1992. Wavelet analysis of backscattering data from an open-ended waveguide cavity. IEEE Microw. Guided Wave Lett. 2 (2), 140–142.
Looney, C.G., 1997. Pattern Recognition Using Neural Networks. Oxford University Press, NewYork.
Mallat, S., 1989. Multifrequency channel decomposition of images and wavelets. IEEE Trans. Acoust. Speech Signal Process 37, 2091–2110.
Mallat, S., Hwang, W.L., 1992. Singularity detection and processing with wavelets. IEEE Tran. Inf. Theory 38 (2), 617–643.
Michalewicz, Z., 1992. Genetic Algorithms + Data Structures = Evolution Programs, 3rd ed. Springer-Verlag.
Misra, K.B., Sharma, U., 1991. An efficient algorithm to solve integer programming problems arising in system reliability design. IEEE Trans. Reliability 40, 81–91.
Mitchell, M., 1996. An Introduction to Genetic Algorithms. MIT Press, Cambridge, MA.
Motlaghi, S., et al., 2008. An expert system design for a crude oil distillation column with the neural networks model and the process optimization using genetic algorithm framework. Expert Syst. Appl. 35 (4), 1540–1545.
Paris, J.L., Pierreval, H., 2001. A distributed evolutionary simulation optimization approach for the configuration of multiproduct kanban systems. Int. J. Comput. Integr. Manuf. 14, 421–430.
Peng, H., Ling, X., 2008. Optimal design approach for the plate-fin heat exchangers using neural networks cooperated with genetic algorithms. Appl. Therm. Eng. 28 (5–6), 642–650.
Qian, Y.B., et al., 1994. Experimental study of heat transfer in vertical annulus during transition boiling. Nucl. Sci. Eng. 14 (3), 213–225.
Ragheb, H.S., Cheng, S.C., 1979. Surface wetted area during transition boiling in forced convective flow. J. Heat Transfer 101, 381–383.
Ragheb, H.S., et al., 1981. Observations in transition boiling of subcooled water under forced convective conditions. Int. J. Heat Mass Transfer 24, 1127–1137.
Sahoo, G.B., Ray, C., 2006. Predicting flux decline in crossflow membranes using artificial neural networks and genetic algorithms. J. Membr. Sci. 283 (1–2), 147–157.
Shang L., et al., 2001. Analysis and identification of HDVC system faults using wavelet modulus maxima. In: Proc. IEE Conference AC-DC Power Transmission, pp. 315–320.
Shen, Q., et al., 1998. Using modulus maximum pair of wavelet transform to detect spike wave of epileptic EEG. In: Proc. 20th Annu. Int. Conf. IEEE 3, pp. 1543–1545.
Shin, T., Han, I., 2000. Optimal signal multi-resolution by genetic algorithms to support artificial neural networks for exchange-rate forecasting. Expert Syst. Appl. 18 (4), 257–269.
Shopova, E.G., Vaklieva-Bancheva, N.G., 2006. BASIC—a genetic algorithm for engineering problems solution. Comput. Chem. Eng. 30, 1293–1309.
Wang, B.X., et al., 2000. Experimental study on the dryout heat flux of falling liquid film. Int. J. Heat Mass Transfer 43, 1897–1903.
Wang, S.T., Seban, R.A., 1988. Heat transfer during the quench process that occurs in the refold of a single vertical tube. Int. J. Heat Mass Transfer 31, 1189–1198.
Xu J.L., A genetic neural network for predicting materials mechanical properties, Third International Conference on Natural Computation (ICNC 2007) 1 (2007) pp. 710–714.
Yue, Q.Y., et al., 2009. Fault line detection of non-effectively earthed neutral system based on modulus maximum determining polarity. In: Power and Energy Engineering Conference, 2009. APPEEC 2009. Asia-Pacific, pp. 1–4.